



Periodic solution for nonlinear vibration of a fluid-conveying carbon nanotube, based on the nonlocal continuum theory by energy balance method

P. Soltani*, A. Farshidianfar

Department of Mechanical Engineering, Ferdowsi University of Mashhad, Mashhad, Iran

ARTICLE INFO

Article history:

Received 7 January 2011

Received in revised form 14 October 2011

Accepted 2 November 2011

Available online 10 November 2011

Keywords:

Flow-induced vibration

Nonlinear vibration

Energy balance method

Nonlocal theory

Pasternak foundation

ABSTRACT

A nonlinear model is developed for the vibration of a single-walled carbon nanotube (SWCNT) based on Eringen's nonlocal elasticity theory. The nanotube is assumed to be embedded in a Pasternak-type foundation with simply supported boundary conditions. The nonlinear equation of motion is solved by the energy balance method (EBM) to obtain a sufficiently accurate flow-induced frequency. It is demonstrated that the nonlinearity of the model makes a reasonable change to the frequency at high flow velocity and for the large deformations. Furthermore, the deviation of the frequency from the linear frequency will be exaggerated with an increase in the nonlocal parameter and a decrease of the Pasternak parameters. Ultimately, the results show that the nonlinearity of the model can be effectively tuned by applying axial tension to the nanotube.

© 2011 Elsevier Inc. All rights reserved.

1. Introduction

The exceptional and extraordinary mechanical, electrical, chemical and physical properties of carbon nanotubes (CNTs) have made them suitable for many innovative applications in nanotechnology. Recently, CNTs have been introduced and used widely as a building block in nano-electro-mechanical systems (NEMS) such as in nano-sensors [1–3], nano-resonators [4,5], nano-switches [6], nano-resistors [7], nano-motors [8] and nano-robots [9]. Moreover, pursuant to hollow cylindrical shape of nanotubes with extremely high elasticity and flexibility, CNTs are used as nano-pipes, nano-containers, and nano-fluid and -gas storage devices [10–13]. In this way, they can be used in nano-medicine as pharmaceutical excipients for creating versatile drug delivery systems (DDSs) [14]. The drug can be delivered directly to the target cells through CNT-based nano-pipes and consequently, the therapeutic properties of the drug will be improved, with a reduction of undesirable side effects [14,15]. In such nanotube-based fluidic devices, flow-induced vibration of CNTs is a very important topic and of great interest to nano-material scientists. Two different approaches are usually applied to investigate the vibrational behavior of nanotubes, namely: the Molecular Dynamic (MD) simulation and the continuum approach. Since MD simulation is still time consuming and needs much computational effort, even for small nano-structures, continuum theories are widely and successfully used to simulate the dynamical behavior of CNTs. The Euler–Bernoulli elastic theory is employed to assess the flow-induced vibrational behavior and stability of single-walled carbon nanotubes (SWCNTs) [16–19] and multi-walled carbon nanotubes (MWCNTs) [15,20–23]. However, as the size of nanotubes is on the nano-scale, the local continuum theories may not predict the mechanical behavior of CNTs accurately. Hence, the nonlocal continuum theory introduced by Eringen [24], which contains information about the long-range forces between atoms and the internal length scale, will be a good

* Corresponding author.

E-mail addresses: payam.soltani@gmail.com, soltanip2@asme.org (P. Soltani).

alternative theory because it provides a more than satisfactory model [25,26]. In recent years, several investigations applied the nonlocal Euler–Bernoulli elastic theory to simulate the vibration of nanotubes conveying fluid. Lee and Chang [27] developed a nonlocal Euler–Bernoulli elastic model of a SWCNT conveying fluid to analyze the effects of the fluid flow on vibration frequency and mode shapes of the nanotube. These authors [28] also considered flow-induced vibration of a viscous-fluid-conveying SWCNT embedded in a Winkler-type foundation, on the basis of the nonlocal continuum theory. The influences of the nonlocal parameter, viscosity, aspect ratio, and elastic medium constant on the fundamental frequency have been investigated. Wang [29] introduced a nonlocal Euler–Bernoulli elastic beam model to describe the vibration and instability of tubular micro- and nano-beams conveying fluid. He found that the effects of the small-scale parameter on vibration properties and critical flow velocity are visible in nano-pipes while such effects can be neglected in micro-pipes. Based on thermal elasticity–mechanics and nonlocal continuum theory, an elastic beam model was developed for analysis of dynamic behavior of fluid-conveying SWCNTs by Zhen and Fang [25]. In this study, the thermal and nonlocal effect on the vibration and instability of a SWCNT conveying fluid was studied. It was found that the natural frequencies and critical flow velocity increase with temperature changes and the nonlocal effect is enhanced with flow velocity.

Since CNTs should usually be embedded in a foundation, the mechanical properties of the medium play an important role in the dynamic behavior of nanotubes. The Winkler-type foundation which simulates the elastic medium as a series of closely spaced, mutually independent, vertical springs is applied widely to show the interaction between the foundation and the CNT [19,25,30–33]. However, this model simulates the foundation as a discontinuous and incoherent medium and cannot predict the mechanical behavior accurately. The Pasternak-type foundation model represents a more precise and generalized simulation of the medium, using two different parameters (called Pasternak parameters). The first parameter represents normal pressure while the second accounts for shear resistance due to interaction of shear deformation of the elastic medium [34]. Recently, the Pasternak-type foundation was applied for vibration analysis of nanotubes [34,35] whereas up to now there was no publication dealing with flow-induced vibration of CNTs using this kind of foundation model.

All of the mentioned works suggested linear formulations for the vibration of CNTs while previous theoretic and experimental investigations [36–38] showed that the deformation of nanostructures, such as CNTs, is nonlinear in nature when subjected to large external loads and displacements. Recently, Rasekh and Khadem [39] developed a nonlinear vibration model of a SWCNT conveying fluid. The SWCNT was assumed to be embedded in a Winkler-type elastic foundation. The nonlinear governing equation of motion was derived using local continuum theory and solved by a traditional perturbation method called the method of multiple scales (MMS). The most important limitation of the perturbation techniques is that the solution is completely related to the small perturbation parameter and is valid for weak nonlinear problems. To obtain the analytical solution for strongly nonlinear models, the approximate variational methods, as novel and simple techniques with reasonable accurate results, can be used instead of traditional perturbation methods. Lately, the approximate variational methods such as the variational iteration method [40–43], the homotopy perturbation method [44–47], the parameter expansion method [48–50], the max–min method [51–53], and the energy balance method [54–58] (EBM) have been widely and successfully applied to various kinds of nonlinear mathematical, physical, and engineering problems. Moreover, in the field of nanostructures and nano-modeling, some research has used approximate variational methods to predict the nonlinear mechanical behavior of nanostructures [59,60].

In this research, for the first time, the nonlocal continuum theory is applied to simulate the nonlinear vibration of a SWCNT conveying fluid, resting on a Pasternak-type elastic foundation. The EBM is used to calculate the nonlinear flow-induced frequency as a function of vibration amplitude. The obtained results show good agreement with the numerical simulation and also with a previous simpler study. The influence of the vibration amplitude, flow velocity, nonlocal parameter and stiffness of the medium on the nonlinear frequency variation is discussed widely. Moreover, it is shown that the axial tension of the nanotube can tune the effect of the nonlinearity of the system effectively.

2. The nonlinear model for a single-walled carbon nanotube conveying fluid

Fig. 1 demonstrates a SWCNT conveying fluid, as a hollow cylindrical tube in a Pasternak-type elastic medium. The nanotube is assumed to be simply supported at both ends and the effect of gravity is negligible. As the SWCNT is supposed to be slender, Euler–Bernoulli beam theory is applied to simulate the vibrational behavior in the model.

Using Newton's law, the governing equation of transverse motion of a SWCNT conveying fluid can be expressed as:

$$\frac{\partial Q}{\partial x} = m_c \frac{\partial^2 w}{\partial t^2} + k_e w - k_p \frac{\partial^2 w}{\partial x^2} + F \frac{\partial^2 w}{\partial x^2} + F_w. \quad (1)$$

where x is the axial coordinate, t is the time and $w(x, t)$ is the transverse deflection of the SWCNT. m_c is the mass of the nanotube per unit length; k_e and k_p are Pasternak parameters that usually represent the Winkler and Pasternak constants of the surrounding medium, in that order. Q and F are the transverse shear force and applied axial tension respectively. F_w represents the force per unit length induced by the fluid flow and is given by Ref. [25] as follows

$$F_w = m_f \left(2v \frac{\partial^2 w}{\partial x \partial t} + v^2 \frac{\partial^2 w}{\partial x^2} + \frac{\partial^2 w}{\partial t^2} \right). \quad (2)$$

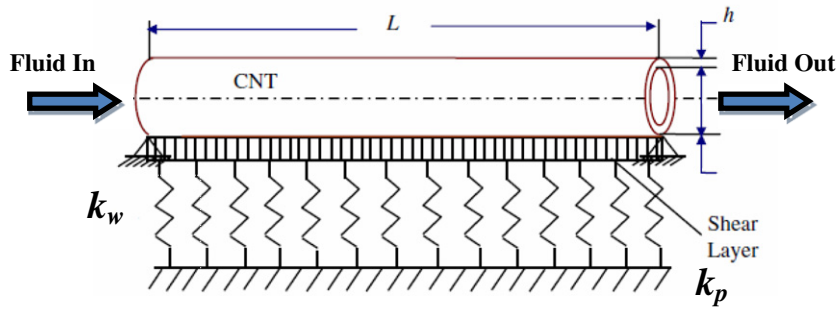


Fig. 1. A single-walled carbon nanotube embedded in a Pastrenak-type foundation model characterized by the Winkler (k_w) and Pasternak (k_p) constant.

Here, v is the uniform mean flow velocity and m_f is the mass of fluid per unit length of a SWCNT. In the above equation, the right terms represent the Coriolis, centrifugal, and transverse forces, in that order.

For Euler–Bernoulli beam theory, the transverse shear force Q , the bending moment of the model M , and the longitudinal force N are related through [61]:

$$\frac{\partial Q}{\partial x} = \frac{\partial^2 M}{\partial^2 x} + N \frac{\partial^2 w}{\partial^2 x}, \tag{3}$$

while the bending moment M and the longitudinal force N can be expressed as

$$M = \int z \sigma_{xx} dA_c = \int z E \epsilon_{xx} dA_c, \quad N = \int \sigma_{xx} dA_c = \int E \epsilon_{xx} dA_c. \tag{4}$$

where ϵ_{xx} and σ_{xx} are the axial strain and the axial stress on the nanotube respectively. z shows the distance from the neutral axis and A_c represents the cross section of the nanotube.

The classical or local continuum theories simulate the mechanical behavior of a structure as continuum medium and state that the stress at a point is only related to the strain state at that point. However, increasing importance of surface energy, discrete nature of the matter, internal strain, and quantum confinement at nanometer length scales may affect this assumption and cause the local continuum theories to cease to be valid for nanostructures [62].

Nonlocal continuum theories, introduced by Eringen in 1983, are concerned with the physics of materials bodies whose behavior at a material point is influenced by the state of all points of the body. These theories are based on lattice dynamics and observations on phonon dispersion that describe the material as consisting of discrete atoms connected by forces from other neighboring atoms. Nonlocal theories state that the stress tensor at a reference point in an elastic medium depends not only on the strains at that point but also on the strains emanating from all other points in the body. This nonlocal description of mechanical behavior of materials is faithful in microscopic scales to the size of the lattice parameter [24] and makes continuum models more accurate on the nanoscale [63]. In other words, the nonlocal elasticity introduces an internal length scale into the constitutive equation as a material parameter and consequently, admits size dependence and small-scale effects in the elastic solutions. From a simple physical point of view, the nonlocal theory introduces a more flexible model as the CNT can be viewed as atoms linked by elastic springs while the local model assumes spring constants to take on an infinite value [64]. The nonlocal constitutive equation for a uniaxial stress state takes the form of [61]:

$$\sigma_{xx} = E \epsilon_{xx} + (e_0 a)^2 \frac{\partial^2 \sigma_{xx}}{\partial x^2}. \tag{5}$$

where E is the Young’s modulus of SWCNT, a is the characteristic length of the structure, and e_0 represents the small scaling parameter. The nonlocal parameter $e_0 a$ in the modeling will lead to a small-scale effect on the response of structures at nano-size and is a constant appropriate to each material which is used for adjusting the model to match reliable results by experimentation or other theories.

Using Eqs. (4) and (5) can be rewritten as:

$$M - (e_0 a)^2 \frac{\partial^2 M}{\partial x^2} = \int z E \epsilon_{xx} dA_c. \tag{6}$$

The two dimensional displacement field of the model is

$$u(x, z, t) = u(x, t) - z \frac{\partial w}{\partial x}, \tag{7a}$$

$$w(x, z, t) = w(x, t). \tag{7b}$$

where u is the longitudinal displacement. The von Karman strain of the Euler–Bernoulli elastic theory [65] associated with the displacement field Eq. (7) is:

$$\varepsilon_{xx} \equiv \frac{\partial u(x, z, t)}{\partial x} + \frac{1}{2} \left(\frac{\partial w(x, z, t)}{\partial x} \right)^2 = \frac{\partial^2 u}{\partial x^2} - z \cdot \frac{\partial^2 w}{\partial x^2} + \frac{1}{2} \left(\frac{\partial w(x, z, t)}{\partial x} \right)^2. \tag{8}$$

Substituting ε_{xx} from Eq. (8) into Eq. (5), we obtain:

$$M - (e_0 a)^2 \frac{\partial^2 M}{\partial x^2} = EI \frac{\partial^2 w}{\partial x^2}. \tag{9}$$

Note that $\int z dA_c = 0$ and $\int z^2 dA_c = I$, where I denotes the second moment of area of the SWCNT about the neutral axis.

Substituting for the second derivative of M from Eq. (3) into Eq. (9), we obtain:

$$M = (e_0 a)^2 \left[\frac{\partial Q}{\partial x} - N \frac{\partial^2 w}{\partial x^2} \right] + EI \frac{\partial^2 w}{\partial x^2}. \tag{10}$$

By substituting M from Eq. (10) into Eq. (9), the dynamical equilibrium equation of the SWCNT will be derived as:

$$EI \frac{\partial^4 w}{\partial x^4} + \frac{\partial Q}{\partial x} - N \frac{\partial^2 w}{\partial x^2} - (e_0 a)^2 \left[\frac{\partial^3 Q}{\partial x^3} - N \frac{\partial^4 w}{\partial x^4} \right] = 0. \tag{11}$$

For slender nanotubes and for immovable end conditions (i.e. $u(0, t) = u(L, t) = 0$), the longitudinal displacement u is expressed as a function of the transverse displacement w and axial tension F [39]

$$u = -\frac{1}{2} \int_0^x \left(\frac{\partial w}{\partial x} \right)^2 dx + x \cdot \left(\frac{F}{EA_c} \right) + \frac{x}{2L} \int_0^L \left(\frac{\partial w}{\partial x} \right)^2 dx. \tag{12}$$

where L is the length of SWCNT.

Substitution of Eqs. (12) and (8) in Eq. (5) yields an explicit expression for the longitudinal force N :

$$N = F + \frac{EA_c}{2L} \int_0^L \left(\frac{\partial w}{\partial x} \right)^2 dx. \tag{13}$$

Substituting Eqs. (1) and (13) into Eq. (11) with using Eq. (2) lead to final form of the nonlinear governing equation of motion of a fluid-conveying SWCNT based on the nonlocal Euler–Bernoulli beam theory:

$$\begin{aligned} m_c \frac{\partial^2 w}{\partial t^2} + EI \frac{\partial^4 w}{\partial x^4} + k_e w - k_p \frac{\partial^2 w}{\partial x^2} + F \frac{\partial^2 w}{\partial x^2} + m_f \left(2v \frac{\partial^2 w}{\partial x \partial t} + v^2 \frac{\partial^2 w}{\partial x^2} + \frac{\partial^2 w}{\partial t^2} \right) \\ - (e_0 a)^2 \left[m_c \frac{\partial^4 w}{\partial t^2 \partial x^2} + k_e \frac{\partial^2 w}{\partial x^2} - k_p \frac{\partial^4 w}{\partial x^4} + F \frac{\partial^4 w}{\partial x^4} + m_f \left(2v \frac{\partial^4 w}{\partial x^3 \partial t} + v^2 \frac{\partial^4 w}{\partial x^4} + \frac{\partial^4 w}{\partial x^2 \partial t^2} \right) - \frac{EA_c}{2L} \cdot \frac{\partial^4 w}{\partial x^4} \cdot \int_0^L \left(\frac{\partial w}{\partial x} \right)^2 dx \right] \\ - \frac{EA_c}{2L} \frac{\partial^2 w}{\partial x^2} \int_0^L \left(\frac{\partial w}{\partial x} \right)^2 dx = 0. \end{aligned} \tag{14}$$

Since the nanotube is assumed to be simply supported at both ends, the boundary conditions can be written as:

$$\begin{aligned} w(0, t) = \frac{\partial^2 w(0, t)}{\partial x^2} = 0 \quad \text{at } x = 0, \\ w(L, t) = \frac{\partial^2 w(L, t)}{\partial x^2} = 0 \quad \text{at } x = L. \end{aligned} \tag{15}$$

In the above formula, $w(x, t)$ are expanded as:

$$w(x, t) = q(t) \cdot \phi_1(x). \tag{16}$$

where ϕ_1 represent the normalized mode functions of the nanotube from the linear vibration analysis due to the specified boundary condition. Meanwhile, the mode function ϕ_1 satisfies the following formula.

$$\int_0^L \phi_i(x) \phi_j(x) dx = \delta_{ij}. \tag{17}$$

and δ_{ij} is the Kronecker delta.

Substituting Eq. (16) into Eq. (14) and utilizing Eq. (17), we have:

$$\ddot{q}(t) + \frac{[1 + e^2(K_e + K_p - T - U^2) + K_e + K_p - T - U^2] \cdot \omega_0^2}{1 + e^2} \cdot q(t) + \frac{\omega_0^2}{4r^2} \cdot q^3(t) = 0. \tag{18}$$

The corresponding dimensionless parameters and variables are defined as:

$$\begin{aligned} \omega_0 &= \frac{\pi^2}{L^2} \sqrt{\frac{EI}{m_c + m_f}}, \quad e = \frac{\pi}{L}(e_0 a), \quad K_e = \frac{L^4}{\pi^4} \frac{1}{EI} k_e, \quad K_p = \frac{L^2}{\pi^2} \frac{1}{EI} k_p, \\ T &= \frac{L^2}{\pi^2} \frac{1}{EI} F, \quad U = \frac{L}{\pi} \sqrt{\frac{m_f}{EI}} \cdot v, \quad r = \sqrt{\frac{I}{A_c}}. \end{aligned} \quad (19)$$

3. Solution procedures

To seek the solution of Eq. (18), we apply EBM to this nonlinear vibration equation. Based on the EBM, the balance between the kinetic and potential energy of a vibrating system occurs when the phase angle of the oscillation is $\frac{\pi}{4}$. Hence, a Hamiltonian is built using the variational principle, and the nonlinear frequency can be determined with the collocation method. [54,66]

The variational form of Eq. (18) can be obtained as:

$$J(q) = \int_0^t \left(-\frac{1}{2} \dot{q}^2(t) + \frac{[1 + e^2(K_e + K_p - T - U^2) + K_e + K_p - T - U^2] \cdot \omega_0^2}{2 \cdot (1 + e^2)} \cdot q^2(t) + \frac{\omega_0^2}{16r^2} q^4(t) \right) dt. \quad (20)$$

If the initial conditions are assumed to be as:

$$q(0) = a_0; \quad \dot{q}(0) = 0. \quad (21)$$

The harmonic approximate solution will be expressed as:

$$q(t) = a_0 \cos(\omega \cdot t). \quad (22)$$

where, ω is the nonlinear flow-induced frequency and a_0 is the amplitude of the vibration.

Therefore, the Hamiltonian of Eq. (20) can be written in the form

$$\begin{aligned} H &= \frac{1}{2} \dot{q}^2(t) + \frac{[1 + e^2(K_e + K_p - T - U^2) + K_e + K_p - T - U^2] \cdot \omega_0^2}{2 \cdot (1 + e^2)} \cdot q^2(t) \\ &+ \frac{\omega_0^2}{16r^2} q^4(t) = \frac{[1 + e^2(K_e + K_p - T - U^2) + K_e + K_p - T - U^2] \cdot \omega_0^2}{2 \cdot (1 + e^2)} a_0^2 + \frac{\omega_0^2}{16r^2} a_0^4. \end{aligned} \quad (23)$$

Or

$$\begin{aligned} H &= \frac{1}{2} \dot{q}^2(t) + \frac{[1 + e^2(K_e + K_p - T - U^2) + K_e + K_p - T - U^2] \cdot \omega_0^2}{2 \cdot (1 + e^2)} \cdot q^2(t) + \frac{\omega_0^2}{16r^2} q^4(t) \\ &= \frac{[1 + e^2(K_e + K_p - T - U^2) + K_e + K_p - T - U^2] \cdot \omega_0^2}{2 \cdot (1 + e^2)} a_0^2 + \frac{\omega_0^2}{16r^2} a_0^4. \end{aligned} \quad (23)$$

By substituting the approximate solution of Eq. (22) into Eq. (24), the following residual will be obtained:

$$\begin{aligned} R(t) &= \frac{1}{2} \cdot (-a_0 \sin(\omega t))^2 + \frac{[1 + e^2(K_e + K_p - T - U^2) + K_e + K_p - T - U^2] \cdot \omega_0^2}{2 \cdot (1 + e^2)} \cdot (a_0 \cos(\omega t))^2 + \frac{\omega_0^2}{16r^2} (a_0 \\ &\times \cos(\omega t))^4 - \frac{[1 + e^2(K_e + K_p - T - U^2) + K_e + K_p - T - U^2] \cdot \omega_0^2}{2 \cdot (1 + e^2)} a_0^2 - \frac{\omega_0^2}{16r^2} a_0^4. \end{aligned} \quad (25)$$

To determine the frequency-amplitude relation, the collocation method should be used in the following form:

$$\int_0^T R(t) \cdot \cos(\omega t) dt = 0; \quad \tau = \frac{\omega}{2\pi}. \quad (26)$$

and the nonlinear frequency ω will be:

$$\omega = \left(\frac{[1 + e^2(K_e + K_p - T - U^2) + K_e + K_p - T - U^2] \cdot \omega_0^2}{(1 + e^2)} + \frac{3 \cdot a_0^2 \cdot \omega_0^2}{16r^2} \right)^{\frac{1}{2}}. \quad (27)$$

The linear resonant frequency ω_L can be obtained from Eq. (25) with $a_0 = 0$

$$\omega_L = \omega|_{a_0=0} = \left(\frac{[1 + e^2(K_e + K_p - T - U^2) + K_e + K_p - T - U^2] \cdot \omega_0^2}{(1 + e^2)} \right)^{\frac{1}{2}}. \quad (28)$$

To show the pure effect of the nonlinearity, “the nonlinear frequency variation” $\% \Delta \omega$ is defined as follows:

$$\% \Delta \omega \equiv \frac{\omega - \omega_L}{\omega_L} \times 100. \quad (29)$$

This parameter demonstrates a more apparent illustration for the difference between the nonlinear and linear model of a CNT conveying fluid and the frequency shift based on the nonlinearity of the CNT.

4. Results and discussion

Fluid flow inside a nanotube plays a role as a source of energy that induces structural and mechanical oscillations. Flow-induced vibrations of a CNT best describe the interaction that occurs between the fluid’s dynamic forces and the nanotube’s inertial, damping, and elastic forces and the simulation of this dynamical behavior is currently a subject of great interest. However, understanding the nature of the flow of liquids at nanoscale is still a very challenging problem and may differ from macro-scale fluid flow. In the nanoscale, the balance of the volume forces is weakened and the impact of the surface forces is enhanced. To this end, the non-slip hypothesis that assumes the zero flow velocity relative to the nanotube at the interface breaks down, and a finite slip velocity of the flow occurs near the nanotube’s wall. This slip boundary condition is one of the marked differences between the macro-scale and the nanoscale flows [67]. Since the continuum approaches represent a generalization of macro-mechanics into nanoscale, the effects of the slip boundary condition are ignored and the obtained results may not exactly reflect the real physics. Thus, these equations should be modified to cover this effect and to represent a more precise continuum model. The Knudsen number K_n is a useful dimensionless criterion which determines whether the fluid flow can be considered as a continuum flow and the non-slip condition is valid. The Knudsen number $K_n \equiv \frac{\lambda}{L^*}$ is defined as the ratio of the molecular mean free path length λ to a representative physical length scale L^* and the magnitude of K_n determines the appropriate flow regime of the fluid through CNT. When the Knudsen number is small and less than 0.01, the flow behaves as a continuous medium and the non-slip condition is established. However, for a nanotube conveying fluid, the Knudsen number is usually greater than 0.01, the slip flow regime occurs near the nanotube’s wall [68], and the continuum models should be modified for solving the nanoscale fluid flow problems. Recently, Rashidi et al. [69] have formulated the small-size effect on slip boundary conditions of nanoflow through the Knudsen number K_n . They found that although the slip boundary regime plays a remarkable role on the vibrational behavior of the CNT conveying nanogas, the non-slip boundary condition can be used in the case of the nanoliquid flow with appropriate accuracy and the fluid can be determined in terms of its macroscopic characteristics.

To evaluate the effects of various parameters on the nonlinear flow-induced frequency of a SWCNT embedded in an elastic medium, the following material and geometrical parameters have been used. The Young’s modulus of the CNT is assumed to be 3.4 Tpa with an effective wall thickness about 0.1 nm, as the recent investigations indicate [70,71]. The inner diameter d_i , the mass density ρ_c and the aspect ratio L/d_i of the SWCNT are 7 nm, 2300 kg/m³, and 20 respectively. The Winkler and Pasternak constant and the axial tension F are set to be zero ($k_w = k_p = F = 0$) and the fluid inside the nanotube is assumed to be that of water with the mass density ρ_f of 1000 kg/m³.

The determination of the magnitude of the nonlocal parameter $e_0 a$ is a key issue in a successful application of the nonlocal continuum models. This value should be calibrated by the generated results from MD simulations for each model separately. Recent investigations [72,73] reveal that this parameter is a function of the boundary conditions, chirality, and the nature of motions in nanotubes. Narendar et al. [73] have conducted a simple molecular structural model to predict the parameter $e_0 a$ in nonlocal continuum shell model of armchair and zigzag SWCNTs under tensile and torsional loadings. They found that the value of the nonlocal parameter is constant and irrespective of the chirality for the nanotubes with large diameters (more than 2 nm) in an axial mode of wave propagation. In a similar work [74], the vibrational behavior of a double-walled carbon nanotube (DWCNT) has been considered and the calibrated nonlocal parameter $e_0 a$ has been proposed by matching the fundamental frequency obtained directly from MD simulation with those calculated via the nonlocal Donnell shell model. It has been observed while the boundary conditions can influence the calibrated nonlocal parameter; chirality has no considerable effect on $e_0 a$. Moreover, a long list of different values of the nonlocal scaling parameter proposed by various researchers can be found in Ref. [75]. This matter shows that the identification of nonlocal parameter $e_0 a$ has not been fully understood and more computational research needs to be conducted in order to evaluate $e_0 a$ more precisely, especially for transverse vibrations of CNTs. In the present study, we choose $e_0 a \leq 2$ nm, as a conservative estimation proposed by Wang and Wang [76].

4.1. Model verification

To verify the accuracy of the model, the dynamic transverse displacement of the SWCNT midpoint is plotted as in Fig. 2. The results are compared with the linear vibration and numerical nonlinear solution of the model on the basis of two different flow velocities ($U = 0.1$ & 0.9). The good adaption between the EBM and numerical results corroborates the validity

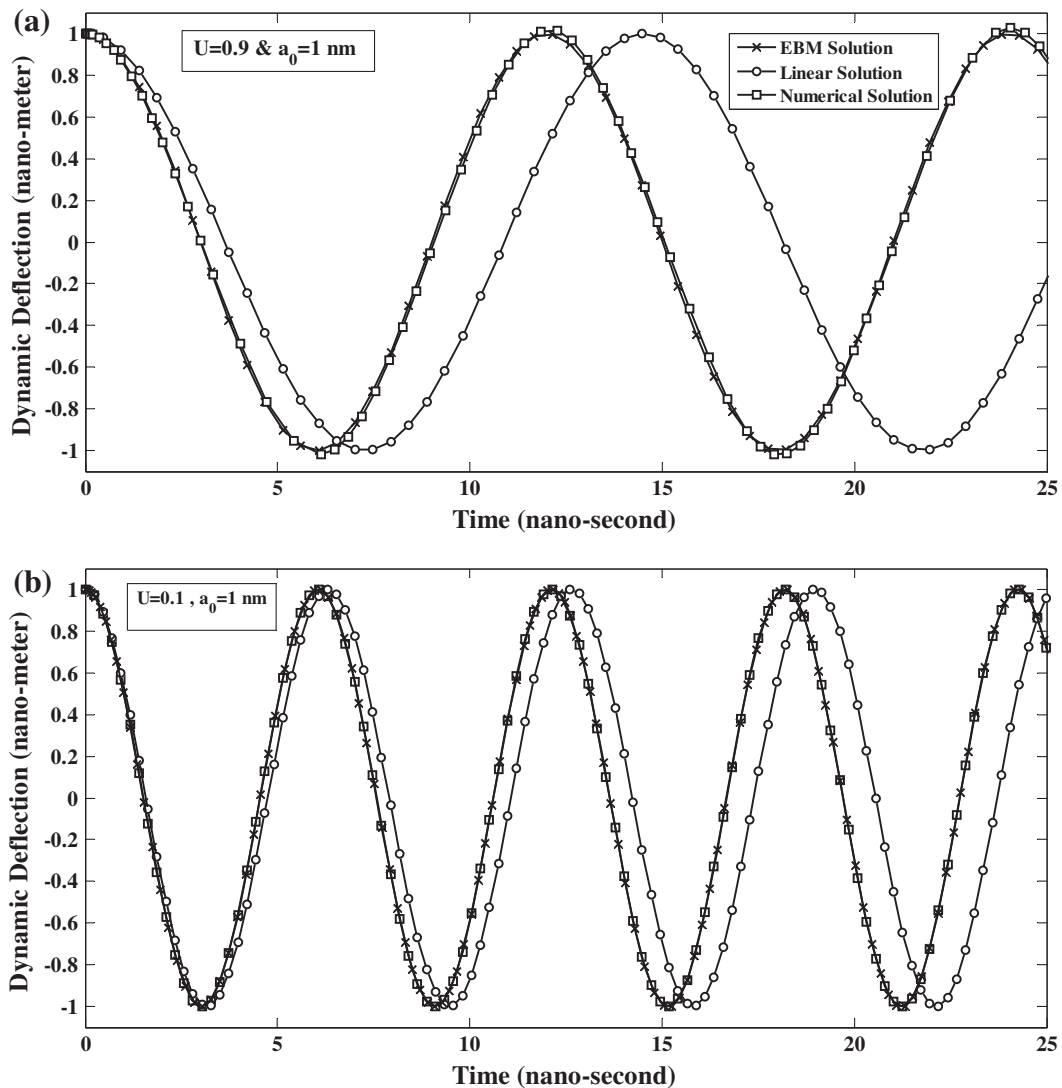


Fig. 2. Comparison between the EBM, linear, and numerical solution (a) at high flow velocity $U = 0.9$ and (b) at low flow velocity $U = 0.1$.

of the energy balance procedure. Moreover, our model predicts a critical flow velocity of 1191.56 m/s for the case study introduced in Ref. [20,39] while the linear numerical approach [20,77] and perturbation method [39] estimate 1190 m/s and 1193 m/s, respectively.

4.2. The nonlinear frequency – amplitude relation

As Eq. (27) shows, the nonlinear flow-induced frequency ω is related to the vibration amplitude a_0 . Hence, in this section, the nonlinear frequency variation $\% \Delta \omega$ is plotted as a function of the vibration amplitude a_0 for some effective parameters in Figs. 3–6. All the figures reveal that the nonlinear frequency variation $\% \Delta \omega$ increases with the vibration amplitude a_0 . In other words, the nonlinear model predicts a higher resonant frequency compared with the linear model, especially for the large amplitudes.

The effect of the nonlocal parameter $e_0 a$ on the nonlinear resonant frequency variation $\% \Delta \omega$ is shown in Fig. 3 with respect to the vibration amplitude a_0 . The figure reveals that the nonlocal model (i.e. $e_0 a \neq 0$) predicts a higher nonlinear frequency in comparison with the local model (i.e. $e_0 a = 0$). In addition, the nonlinear frequency increases with an increase of the nonlocal parameter $e_0 a$. As mentioned above, the nonlocal theory introduces a more flexible model and with increasing the flexibility, the effect of the nonlinearity on the model becomes more significant, which describes why $\% \Delta \omega$ rises with the nonlocal parameter $e_0 a$.

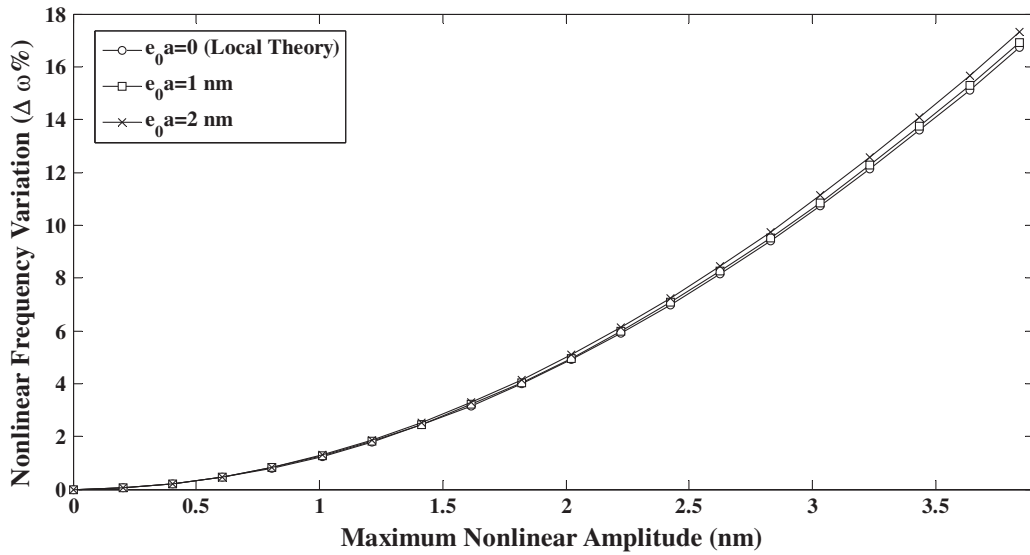


Fig. 3. The nonlinear frequency variation $\% \Delta\omega$ against the maximum nonlinear amplitude a_0 with various nonlocal parameters e_0a .

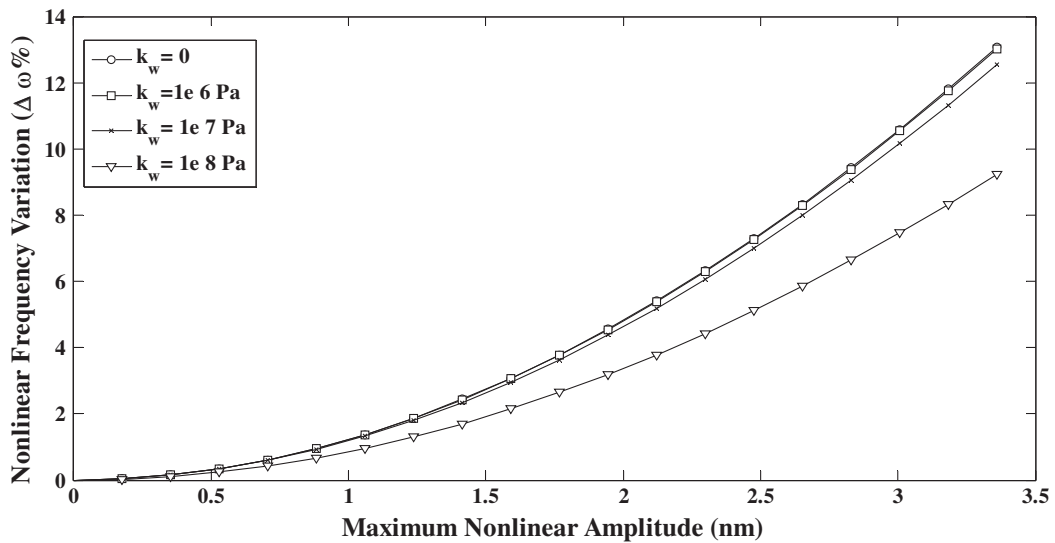


Fig. 4. The nonlinear frequency variation $\% \Delta\omega$ against the maximum nonlinear amplitude a_0 with various Winkler constants k_w ($e_0a = 1$ nm).

The mechanical properties of the elastic medium around the nanotube are another important factor directly affects the resonant frequency. As mentioned above, the foundation of the SWCNT is assumed as in the Pasternak model. The Pasternak-type foundation, that is also called the two-parameter foundation model, simulates the interaction between the medium and the nanotube using two different parameters. The first parameter of the Pasternak foundation model k_w represents normal pressure, while the second parameter k_p accounts for transverse shear stress due to the interaction of shear deformation of the surrounding elastic medium [35]. These factors k_w and k_p are called the Winkler and Pasternak constants, respectively.

The effects of the Pasternak parameters on the nonlinear frequency are shown in Figs. 4 and 5. Fig. 4 shows the effect of the Winkler constant k_w on the nonlinear frequency variation $\% \Delta\omega$. As can be seen, with an increase in the Winkler constant k_w , the parameter $\% \Delta\omega$ decreases, especially for small vibration amplitudes a_0 . This means that as the nanotube vibrates in a stiff medium, the nonlinear frequency tends to the linear frequency. In other words, for stiff elastic foundations and in small amplitudes, the linear simulation of the SWCNT represents a sufficiently accurate theoretical model for transverse flow-induced vibrations. The shear resistance of the surrounding elastic medium and its corresponding interaction on the nanotube is characterized by the Pasternak constant k_p . Fig. 5 plots the nonlinear frequency variation $\% \Delta\omega$ as a function

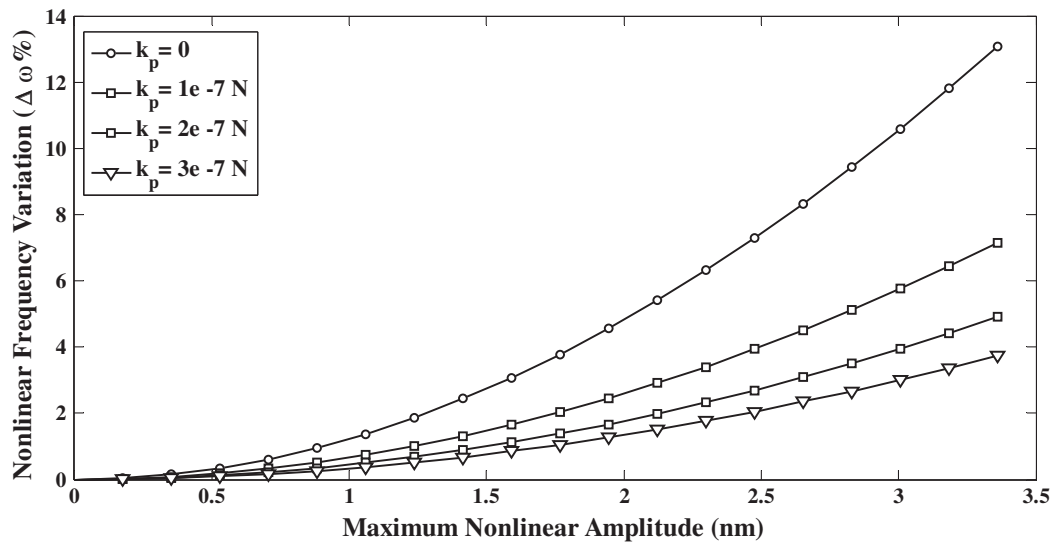


Fig. 5. The nonlinear frequency variation $\% \Delta \omega$ against the maximum nonlinear amplitude a_0 with various Pasternak constants k_p ($e_0 a = 1$ nm).

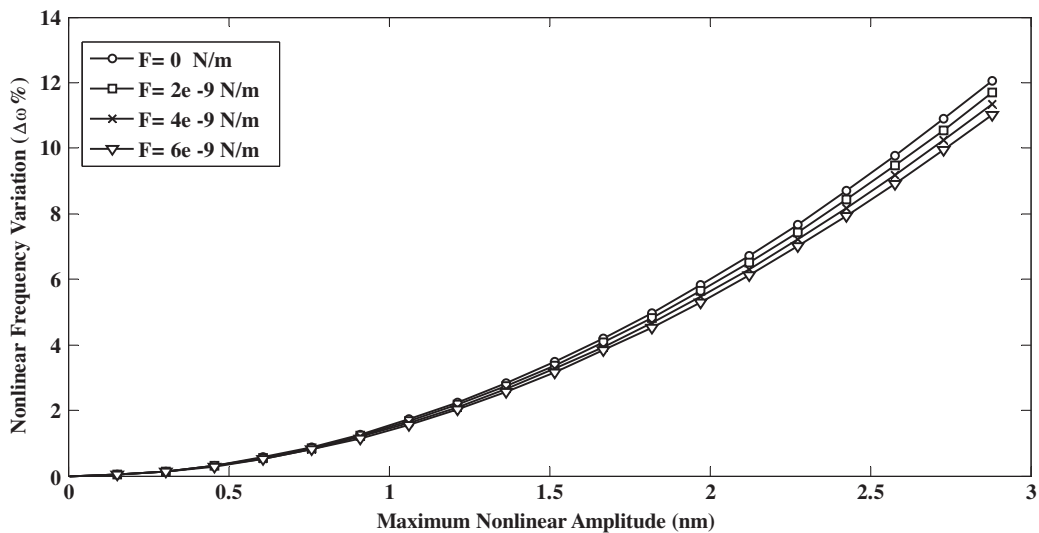


Fig. 6. The nonlinear frequency variation $\% \Delta \omega$ against the maximum nonlinear amplitude a_0 with various axial tensions F ($e_0 a = 1$ nm).

of k_p and the vibration amplitude a_0 . The figure indicates that as the shear stiffness of the medium increases and for the small vibration amplitudes, the parameter $\% \Delta \omega$ decreases, and the nonlinear flow-induced frequency reduces to the linear frequency.

Axial tension induced through external electrical fields tunes the vibration of CNTs in NEMS [78]. In fluid-conveying CNTs, axial tension increases the stiffness of the model and can limit the flow-induced vibration and nonlinearity of the system. The effect of the axial tension F on the nonlinear frequency variation $\% \Delta \omega$ is illustrated in Fig. 6. The results indicate that axial tension of the SWCNT can reduce the difference between the nonlinear and the linear resonant frequency, and this effect is profound for high vibration amplitude a_0 . In other words, the nonlinearity can be controlled by increasing the axial tension F .

4.3. The nonlinear frequency- flow velocity relation

The resonant frequency of the SWCNT conveying fluid is affected by the fluid flow within the nanotube and the kinetic energy of the fluid flow is an essential issue in causing the nanotube to vibrate. In this section, the nonlinear frequency variation $\% \Delta \omega$ is plotted against the dimensionless fluid flow velocity U for some parameters (Figs. 7–10). In all these figures, it

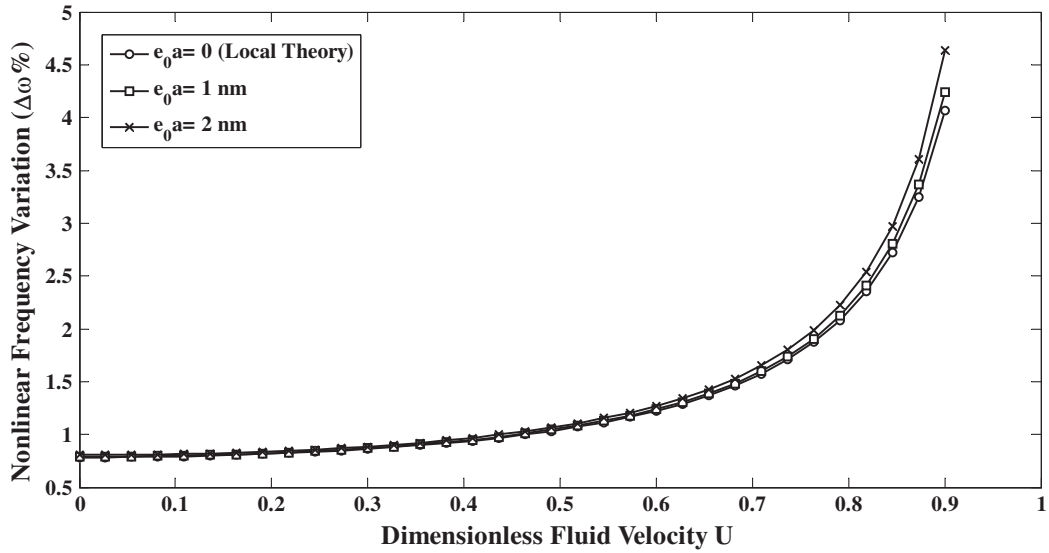


Fig. 7. The nonlinear frequency variation $\% \Delta \omega$ against the dimensionless fluid velocity U with various nonlocal parameters $e_0 a$.

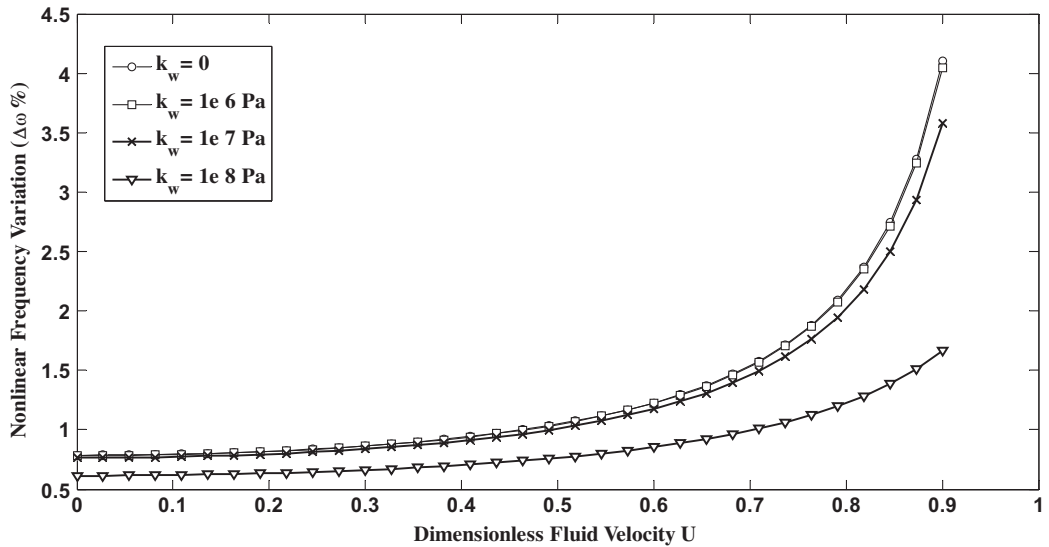


Fig. 8. The nonlinear frequency variation $\% \Delta \omega$ against the dimensionless fluid velocity U with various Winkler constants $k_w (e_0 a = 1 \text{ nm})$.

is clear that the nonlinear frequency variation $\% \Delta \omega$ shifts upwards with fluid velocity and the nonlinearity of the model makes a meaningful difference between linear and nonlinear frequency at high flow velocities. Fig. 7 represents the effect of the nonlocal parameter $e_0 a$ on the nonlinear frequency variation $\% \Delta \omega$ with flow velocity. The results indicate that at low fluid velocities ($U < 0.5$), the effects of the nonlocal parameter is not significant and the nonlinear frequency variation $\% \Delta \omega$ is not related to the small-scale parameters; while at higher flow velocities, the nonlinear frequency increases with respect to the linear frequency, especially when the nonlocal parameter $e_0 a$ increases. The effects of the Winkler constant k_w on the nonlinear frequency variation $\% \Delta \omega$ with regard to the flow velocity are shown in Fig. 8. As shown in the figure, the mediums with stiff elastic properties cause the difference between the nonlinear and linear frequency to remain unchanged with respect to flow velocity and $\% \Delta \omega$ remains almost constant at low fluid velocities ($U < 0.5$). Moreover, for compliant mediums with $k_w < 1e7 \text{ Pa}$, the nonlinear frequency variation $\% \Delta \omega$ increases with the flow velocity and this pattern is amplified by decreasing the Winkler constant k_w . Fig. 9 displays the nonlinear frequency variation $\% \Delta \omega$ with the dimensionless flow velocity U for some Pasternak constants k_p . It is observed that at low fluid velocities ($U < 0.5$) and as the shear stiffness of the elastic medium increases, $\% \Delta \omega$ declines to less than 0.8% and remains constant with any increase of the flow

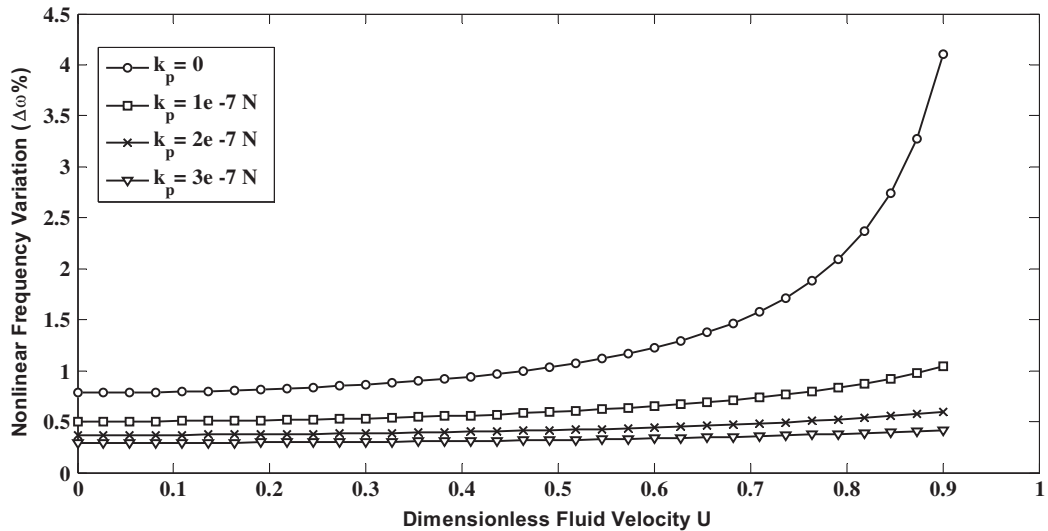


Fig. 9. The nonlinear frequency variation $\% \Delta \omega$ against the dimensionless fluid velocity U with various Pasternak constants k_p ($e_0 a = 1$ nm).

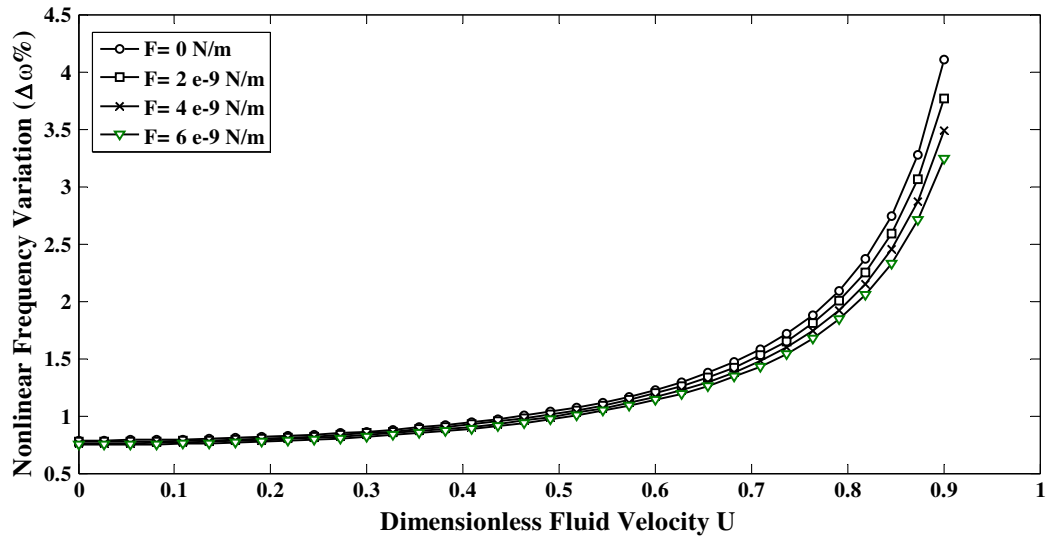


Fig. 10. The nonlinear frequency variation $\% \Delta \omega$ against the dimensionless fluid velocity U with various axial tensions F ($e_0 a = 1$ nm).

velocity. This shows that the nonlinear vibration behavior of the SWCNT is independent of the fluid flow and can be disregarded for mediums with high shear strength.

Fig. 10 reveals that the axial tension F has no significant effect on the nonlinear frequency variation $\% \Delta \omega$ at low flow velocities ($U < 0.4$). However, at high flow velocity, the parameter $\% \Delta \omega$ decreases with F and the nonlinearity effect can be controlled by tuning the axial tension on the model.

5. Conclusion

The nonlinear vibration model of a fluid-conveying SWCNT embedded in a Pasternak foundation was derived on the basis of the nonlocal continuum theory. The energy balance method was applied successfully to the nonlinear governing equation of motion, and an analytical solution was obtained for the nonlinear flow-induced frequency. The accuracy of the results was verified with the numerical approach and a previous simpler model. The results show that the deviation of the nonlinear flow-induced frequency from the linear frequency is considerable when the amplitude, flow velocity, and nonlocal parameter are high while for the CNTs embedded in the mediums of high Pasternak parameters, the nonlinearity of the model does

not demonstrate a significant effect on the frequency. Moreover, the axial tension restricts the nonlinear effect and limits the flow induced-vibration of the nanotube at high flow velocity and for high vibration amplitudes.

References

- [1] A.Y. Joshi, S.P. Harsha, S.C. Sharma, *Physica E* 42 (2010) 2115–2123.
- [2] S. Roy, Z. Gao, *Nano Today* 4 (2009) 318–334.
- [3] S.S. Hosseini Yazdi, M. Mousavi Mashadi, *J. Appl. Sci.* 7 (2007) 1442–1445.
- [4] E. Mile, G. Jourdan, I. Bargatin, S. Labarthe, C. Marcoux, P. Andreucci, S. Hentz, C. Kharrat, E. Colinet, L. Duraffourg, *Nanotechnology* 21 (2010).
- [5] Y.W. Kwon, C. Manthena, J.J. Oh, D. Srivastava, *J. Nanosci. Nanotechnol.* 5 (2005) 703–712.
- [6] S. Lee, *J. Korean Phys. Soc.* 55 (2009) 957–961.
- [7] A.G.N.Yu.E. Lozovik, A.M. Popov, *J. Exp. Theor. Phys.* 103 (2006) 449–462.
- [8] M. Hamdi, A. Subramanian, L.X. Dong, A. Ferreira, B.J. Nelson, in: *Anchorage, AK, 2010*, pp. 1586–1591.
- [9] R.A. Freitas Jr, *J. Comput. Theor. Nanosci.* 2 (2005) 1–25.
- [10] M. Whitby, N. Quirke, *Nat Nano* 2 (2007) 87–94.
- [11] S.S. Hosseini Yazdi, M.M. Mashadi, *J. Appl. Sci.* 7 (2007) 715–719.
- [12] S. Babu, P. Ndungu, J.C. Bradley, M.P. Rossi, Y. Gogotsi, *Microfluid. Nanofluid.* 1 (2005) 284–288.
- [13] A.V. Melechko, T.E. McKnight, M.A. Guillorn, B. Ilic, V.I. Merkulov, M.J. Doktycz, B. Warmac, D. McCorkle, D.H. Lowndes, M.L. Simpson, in 2003, pp. 416–419.
- [14] F. Marianna, B. Mukasa, *Nanomed. Nanotechnol. Biol. Med.* 4 (2008) 183–200.
- [15] N. Khosravian, H. Rafii-Tabar, *Nanotechnology* 19 (2008).
- [16] C.D. Reddy, C. Lu, S. Rajendran, K.M. Liew, *Appl. Phys. Lett.* 90 (2007).
- [17] C.D. Reddy, C. Lu, *J. Appl. Phys.* 103 (2008).
- [18] L. Wang, Q. Ni, *Comput. Mater. Sci.* 43 (2008) 399–402.
- [19] T. Natsuki, Q.Q. Ni, M. Endo, *J. Appl. Phys.* 105 (2009).
- [20] J. Yoon, C.Q. Ru, A. Mioduchowski, *Compos. Sci. Technol.* 65 (2005) 1326–1336.
- [21] J. Yoon, C.Q. Ru, A. Mioduchowski, *Int. J. Solids Struct.* 43 (2006) 3337–3349.
- [22] N. Khosravian, H. Rafii-Tabar, *J. Phys. D Appl. Phys.* 40 (2007) 7046–7052.
- [23] Y. Yan, W.Q. Wang, L.X. Zhang, *Appl. Math. Model.* 33 (2009) 1430–1440.
- [24] A.C. Eringen, *J. Appl. Phys.* 54 (1983) 4703–4710.
- [25] Y. Zhen, B. Fang, *Comput. Mater. Sci.* 49 (2010) 276–282.
- [26] Q. Wang, K.M. Liew, *Phys. Lett., Section A: General, Atomic Solid State Phys.* 363 (2007) 236–242.
- [27] H.L. Lee, W.J. Chang, *J. Appl. Phys.* 103 (2008).
- [28] H.L. Lee, W.J. Chang, *Physica E* 41 (2009) 529–532.
- [29] L. Wang, *Physica E* 41 (2009) 1835–1840.
- [30] X. Wang, X.Y. Wang, G.G. Sheng, *J. Phys. D Appl. Phys.* 40 (2007) 2563–2572.
- [31] K.M. Liew, X.Q. He, S. Kitipornchai, *Proc. Roy. Soc. A: Math. Phys. Eng. Sci.* 461 (2005) 3785–3805.
- [32] T. Murmu, S.C. Pradhan, *Comput. Mater. Sci.* 47 (2010) 721–726.
- [33] T. Natsuki, X.W. Lei, Q.Q. Ni, M. Endo, *Phys. Lett., Section A: General, Atomic Solid State Phys.* 374 (2010) 2670–2674.
- [34] T. Murmu, S.C. Pradhan, *Physica E* 41 (2009) 1232–1239.
- [35] S.C. Pradhan, T. Murmu, *J. Appl. Phys.* 105 (2009).
- [36] D. Walgraef, *The European Phys. J. – Special Topics* 146 (2007) 443–457.
- [37] Y.M. Fu, J.W. Hong, X.Q. Wang, *J. Sound Vib.* 296 (2006) 746–756.
- [38] J. Yang, L.L. Ke, S. Kitipornchai, *Physica E* 42 (2010) 1727–1735.
- [39] M. Rasekh, S.E. Khadem, *J. Phys. D Appl. Phys.* 42 (2009).
- [40] J.-H. He, *J. Comput. Appl. Math.* 207 (2007) 3–17.
- [41] J.-H. He, X.-H. Wu, *Chaos, Solitons Fractals* 29 (2006) 108–113.
- [42] P. Rafalski, *Int. J. Eng. Sci.* 13 621–630.
- [43] M. Rafei, D.D. Ganji, H. Daniali, H. Pashaei, *J. Sound Vib.* 305 (2007) 614–620.
- [44] J.-H. He, *Appl. Math. Comput.* 135 (2003) 73–79.
- [45] S.S. Ganji, D.D. Ganji, A.G. Davodi, S. Karimpour, *Appl. Math. Model.* 34 (2010) 2676–2684.
- [46] M. Idrees, S. Islam, S. Haq, S. Islam, *Comput. Math. Appl.* 59 (2010) 3858–3866.
- [47] Z.-F. Ren, J.-H. He, *Phys. Lett. A* 373 (2009) 3749–3752.
- [48] S.-Q. Wang, J.-H. He, *Chaos, Solitons Fractals* 35 (2008) 688–691.
- [49] S.T. Mohyud-Din, M.A. Noor, K.I. Noor, *Int. J. Nonlinear Sci. Numer. Simul.* 10 (2009) 581–583.
- [50] M.T. Darvishi, A. Karami, B.C. Shin, *Phys. Lett., Section A: General, Atomic Solid State Phys.* 372 (2008) 5381–5384.
- [51] J.H. He, *Int. J. Nonlinear Sci. Numer. Simul.* 9 (2008) 207–210.
- [52] D.Q. Zeng, *Chaos, Solitons Fractals* 42 (2009) 2885–2889.
- [53] D.Q. Zeng, Y.Y. Lee, *Int. J. Nonlinear Sci. Numer. Simul.* 10 (2009) 1361–1368.
- [54] J.H. He, *Mech. Res. Commun.* 29 (2002) 107–111.
- [55] J.H. He, *Int. J. Mod. Phys. B* 22 (2008) 3487–3578.
- [56] S.S. Ganji, D.D. Ganji, Z.Z. Ganji, S. Karimpour, *Acta Applicandae Mathematicae* 106 (2009) 79–92.
- [57] N. Jamshidi, D.D. Ganji, *Curr. Appl. Phys.* 10 (2010) 484–486.
- [58] L.B. Ibsen, A. Barari, A. Kimiaefar, *Sadhana – Academy Proc. Eng. Sci.* 35 (2010) 433–448.
- [59] R. Ansari, M. Hemmatnezhad, H. Ramezannezhad, *Numer. Meth. Partial Differ. Eqs.* 26 (2010) 490–500.
- [60] Y. Fu, J. Zhang, L. Wan, *Curr. Appl. Phys.* (2010).
- [61] J.N. Reddy, S.D. Pang, *J. Appl. Phys.* 103 (2008).
- [62] R. Maranganti, P. Sharma, *J. Mech. Phys. Solids* 55 (2007) 1823–1852.
- [63] M. Aydogdu, *Physica E* 41 (2009) 1651–1655.
- [64] A. Tounsi, H. Heireche, H.M. Berrabah, A. Benzair, L. Boumia, *J. Appl. Phys.* 104 (2008).
- [65] J.N. Reddy, *Int. J. Eng. Sci.* 48 (2010) 1507–1518.
- [66] J.H. He, *Appl. Math. Comput.* 151 (2004) 293–297.
- [67] Y. Li, J. Xu, D. Li, *Microfluid. Nanofluid.* 9 (2010) 1011–1031.
- [68] G. Karniadakis, A. Be kök, N.R. Aluru, *Microflows Nanoflows: Fundamentals and Simul.*, Springer Verlag, 2005.
- [69] V. Rashidi, H.R. Mirdamadi, E. Shirani, *Comput. Mater. Sci.* 51 (2012) 347–352.
- [70] R.C. Batra, S.S. Gupta, *J. Appl. Mech.* 75 (2008) 061010–061016.
- [71] C.Y. Wang, L.C. Zhang, *Nanotechnology* 19 (2008) 195704.
- [72] B. Arash, Q. Wang, *Comput. Mater. Sci.* 51 (2012) 303–313.

- [73] S. Narendar, D. Roy Mahapatra, S. Gopalakrishnan, *Int. J. Eng. Sci.* 49 (2011) 509–522.
- [74] R. Ansari, H. Rouhi, S. Sahmani, *Int. J. Mech. Sci.* 53 (2011) 786–792.
- [75] S. Narendar, S. Gopalakrishnan, *Composites Part B* 42 (2011) 2013–2023.
- [76] Q. Wang, C.M. Wang, *Nanotechnology* 18 (2007).
- [77] T. Natsuki, Q.Q. Ni, M. Endo, *Appl. Phys. A: Mater. Sci. Process.* 90 (2008) 441–445.
- [78] X. Wei, Q. Chen, S. Xu, L. Peng, J. Zuo, *Adv. Funct. Mater.* 19 (2009) 1753–1758.